Electronic Supplementary Material (ESI) for Polymer Chemistry

Supporting Information

Synthesis and Characterization of Thermo-responsive Polypeptoid Bottlebrushes

Samuel H. Lahasky, Lu Lu, Wayne A. Huberty, Jinbao Cao, Li Guo, Jayne C. Garno and Donghui Zhang*

Department of Chemistry and Macromolecular Studies Group, Louisiana State University, Baton Rouge, Louisiana 70803, United States.

Corresponds to: dhzhang@lsu.edu

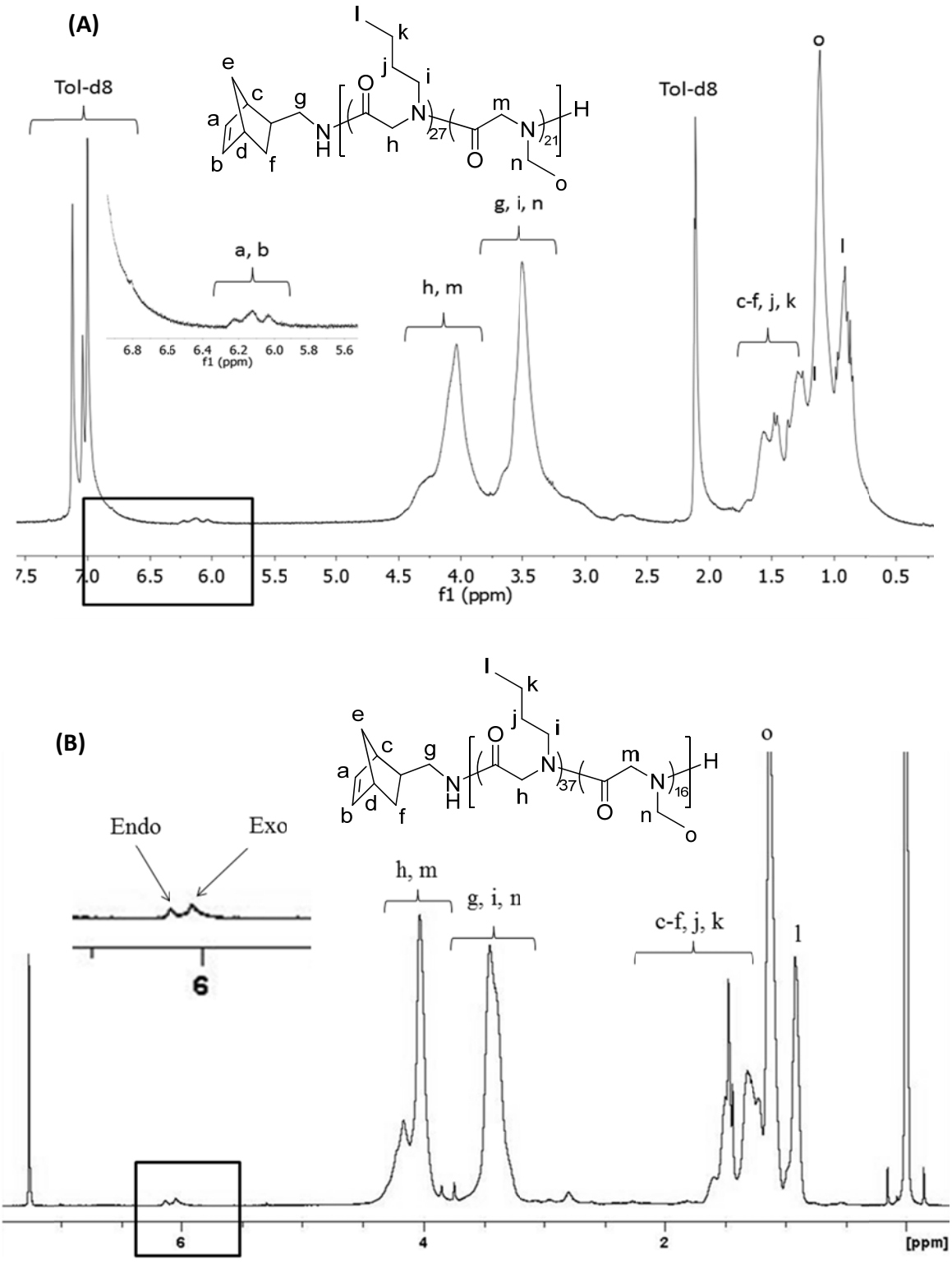

Figure S1. (A) ^{1}H NMR spectra of the Nor-P(NEG$_{27}$-*r*-NBG$_{21}$) macromonomer (Entry 1, Table S1) in toluene-d8 and (B) the Nor-P(NEG$_{37}$-*r*-NBG$_{16}$) macromonomer (Entry 2, Table S1) in $CDCl_3$.

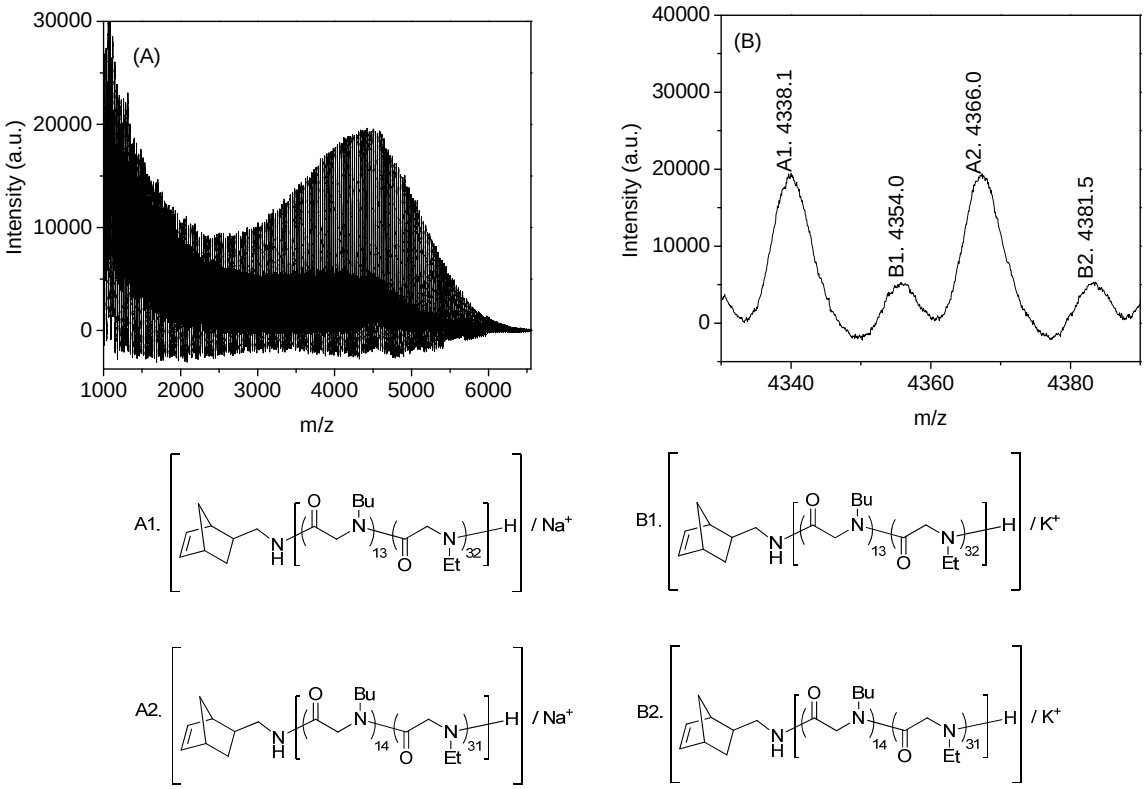

Figure S2. (A) Full and (B) expanded MALDI-TOF MS spectra of a norbornenyl-terminated poly(N-ethyl glycine)-*ran*-poly(N-butyl glycine) random copolymer [Nor-P(NEG_{43}-*r*-NBG_{32})] (M_n = 2.2 kg·mol^{-1}, PDI = 1.40 from MS analysis).

Table S1. The molecular weight and composition of the polypeptoid macromonomers [Nor-P(NEG_n-*r*-NBG_m)$_{n+m}$]

Entry	$[M_1]_0$:$[M_2]_0$:$[I]_0$	Macromonomer composition [a]	M_n (kg·mol^{-1}) [a]	M_n (kg·mol^{-1}) [b]	PDI
1	33:17:1	Nor-P(NEG_{27}-*r*-NBG_{21})	4.7	10.4	1.05
2	38:12:1	Nor-P(NEG_{37}-*r*-NBG_{16})	5.0	10.4	1.04
3	42:8:1	Nor-P(NEG_{36}-*r*-NBG_{12})	4.4	9.8	1.05
4	45:5:1	Nor-P(NEG_{40}-*r*-NBG_9)	4.4	9.7	1.05

[a.] Determined by integration of the ethyl and butyl methyl peaks relative to the norbornenyl methylene peaks in their respective ^{1}H NMR spectra in toluene-d_8; [b.] determined from SEC-MALS-DRI chromatography in 0.1 M LiBr/DMF using polystyrene standards (flow rate = 0.5 mL·min^{-1}).

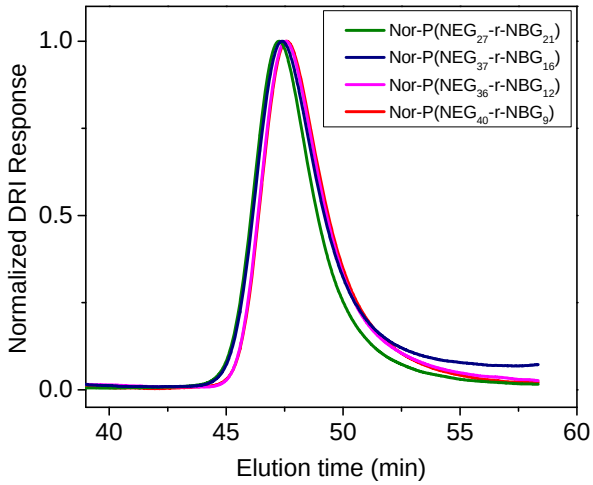

Figure S3. SEC-DRI chromatograms of the polypeptoid macromonomers [Nor-P(NEG_n-*r*-NBG_m)$_{n+m}$] (Entry 1-4, Table S1).

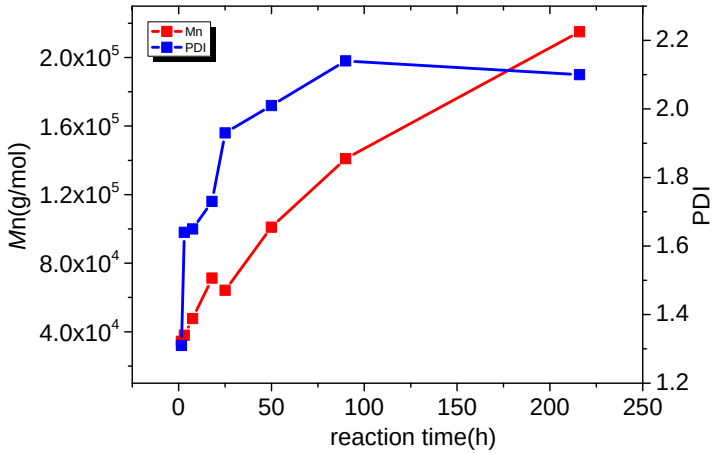

Figure S4. Plots of M_n and PDI versus time for the ROMP reaction of Nor-P(NEG_{40}-*r*-NBG_9) (conditions: $[Nor]_0/[Ru]_0$=150:1, $[Nor]_0$= 0.01M, 40 °C, CH_2Cl_2).

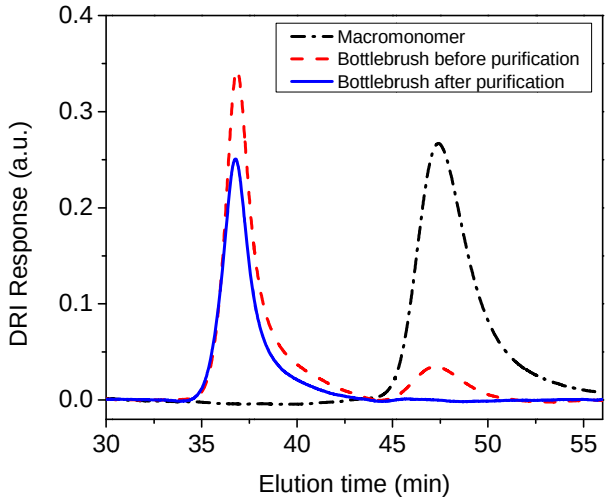

Figure S5. Representative SEC-DRI chromatograms of the polypeptoid macromonomer [Nor-P(NEG$_{37}$-*r*-NBG$_{16}$), -·-] and the corresponding bottlebrush copolymer before (---) and after (—) purification by centrifugal dialysis.

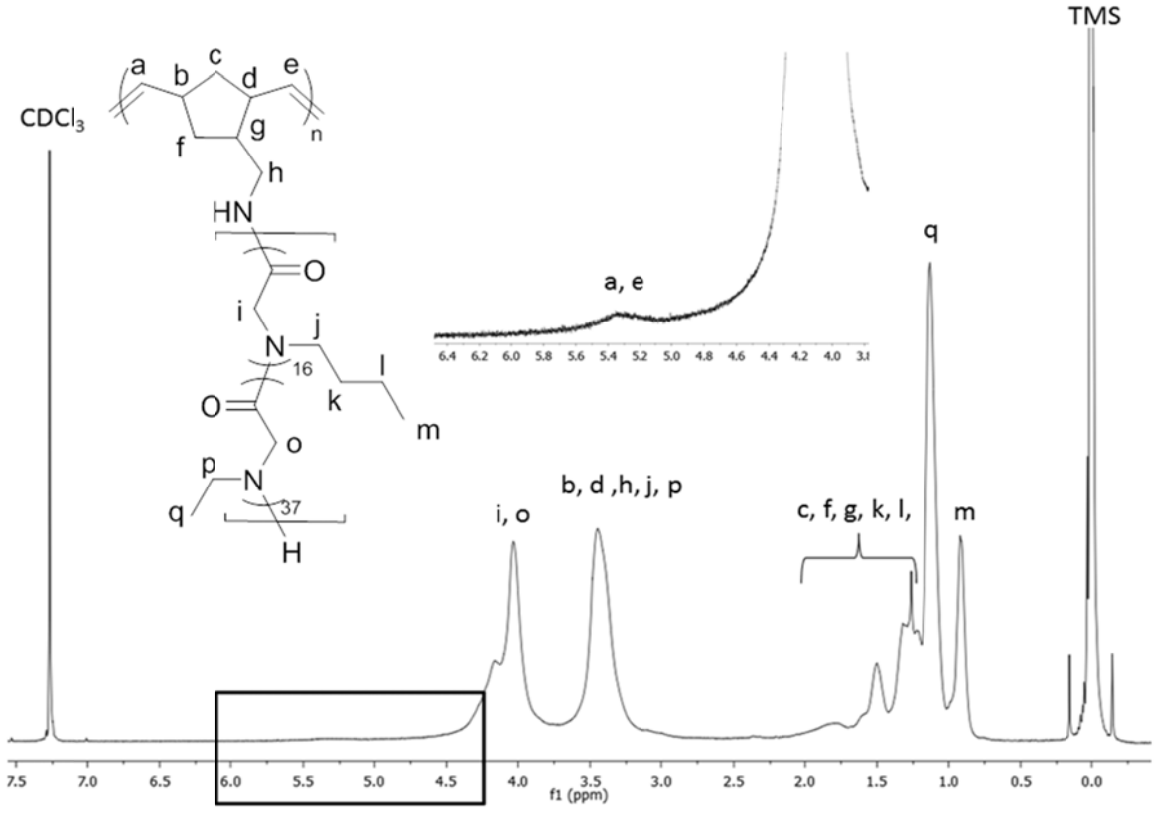

Figure S6. ^{1}H NMR spectrum of the PNor$_{25}$-*g*-P(NEG$_{37}$-*r*-NBG$_{16}$) bottlebrush copolymer (Entry 2, Table 1) in $CDCl_3$.

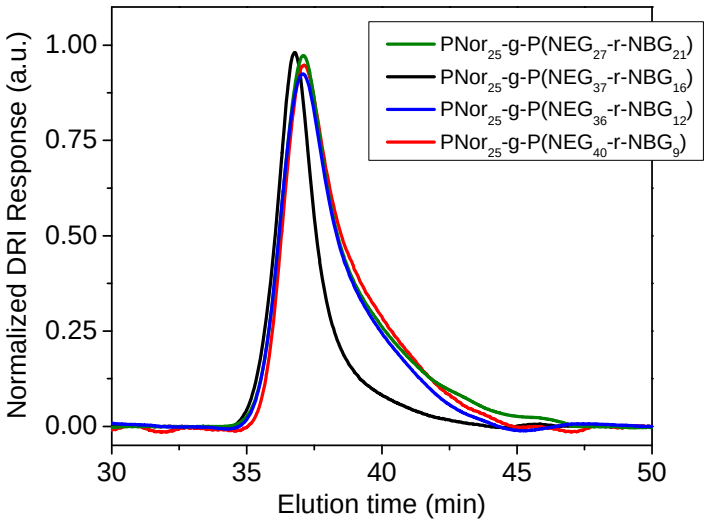

Figure S7. SEC-DRI chromatograms of the polypeptoid bottlebrushes having the same backbone length and various side chain compositions (Entries 1-3 and 5, Table 1).

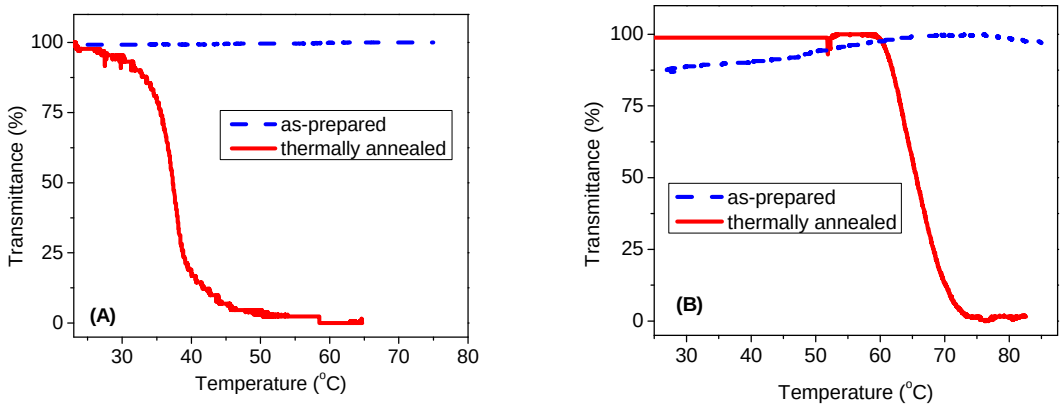

Figure S8. (A) Transmittance versus temperature plots for the as-prepared (---) and thermally annealed aqueous solutions (—) of the bottlebrush copolypeptoid $PNor_{25}$-*g*-P(NEG_{27}-*r*-NBG_{21}) (Entry 1, Table 1) and (B) $PNor_{25}$-*g*-P(NEG_{36}-*r*-NBG_{12}) (Entry 3, Table 1).

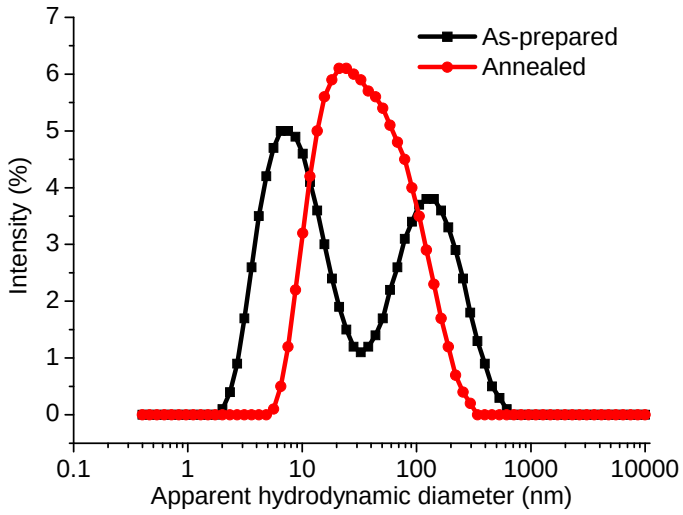

Figure S9. Dynamic light scattering (DLS) analysis of aqueous solutions (1.0 mg·ml^{-1}) containing as-prepared (—) or thermally-annealed PNor$_{25}$-*g*-P(NEG$_{27}$-*r*-NBG$_{21}$) sample (—) (Entry 1, Table 1) at 25 °C.

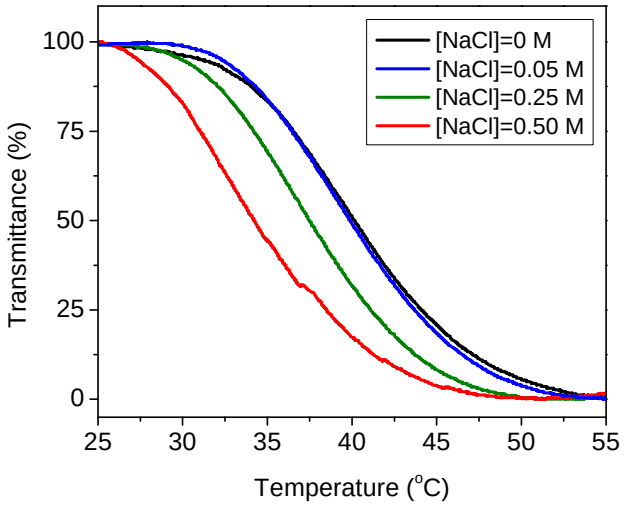

Figure S10. Transmittance versus temperature plots of the polypeptoid macromonomer [Nor-P(NEG$_{27}$-*r*-NBG$_{21}$)] (Entry 1, Table S1) in aqueous solutions with varying NaCl concentrations.

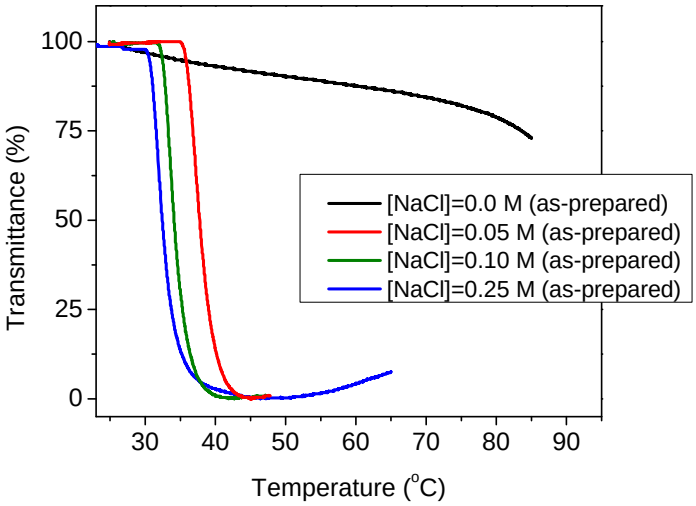

Figure S11. Transmittance versus temperature plot of the polypeptoid bottlebrush [PNor$_{25}$-*g*-P(NEG$_{27}$-*r*-NBG$_{21}$)] (Entry 1, Table 1) in aqueous solutions with varying NaCl concentrations.

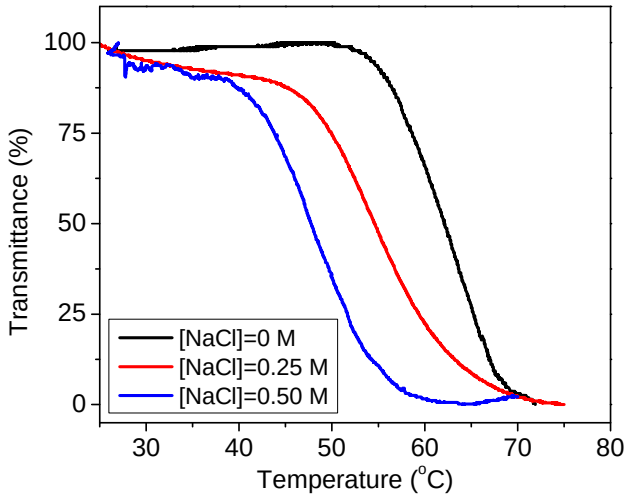

Figure S12. Transmittance versus temperature plots of the polypeptoid macromonomer [Nor-P(NEG$_{37}$-*r*-NBG$_{16}$)] (Entry 2, Table S1) in aqueous solutions with varying NaCl concentrations.

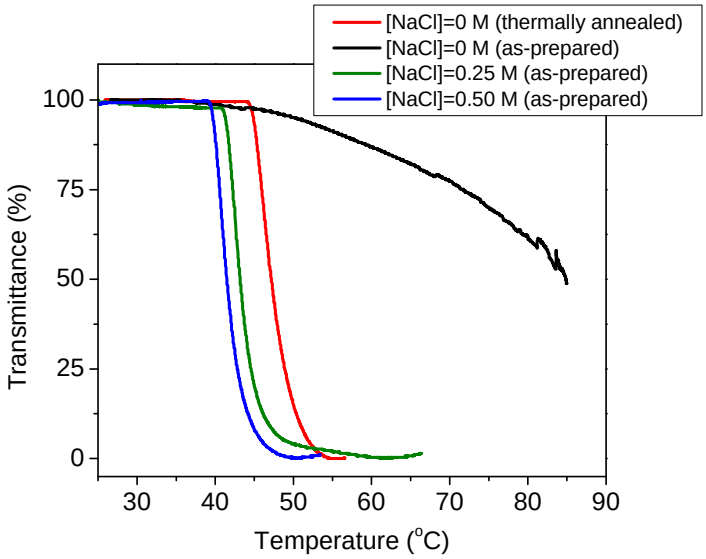

Figure S13. Transmittance versus temperature plots of the polypeptoid bottlebrush [$PNor_{25}$-*g*-$P(NEG_{37}$-*r*-$NBG_{16})$] (Entry 2, Table 1) in aqueous solutions with varying NaCl concentrations. The solutions are either subjected to the turbidity measurement directly (as-prepared) or thermally annealed at 75 °C for 10 min followed by cooling at 4 °C overnight prior to the turbidity measurement.

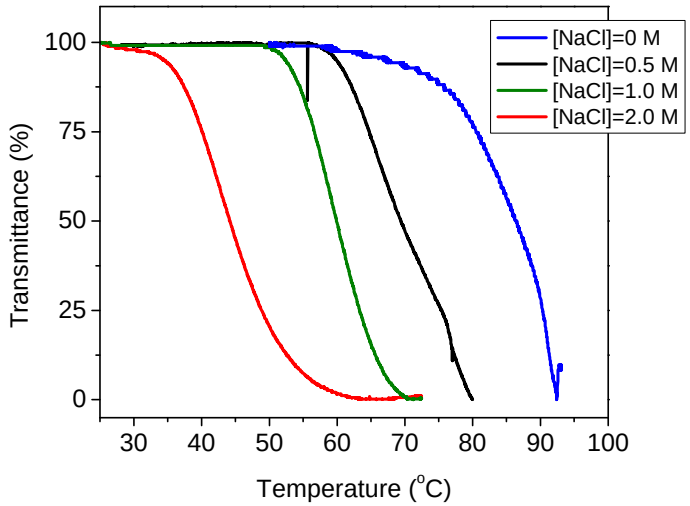

Figure S14. Transmittance versus temperature plots of the polypeptoid macromonomer (Nor-$P(NEG_{36}$-*r*-NBG_{12}) (Entry 3, Table S1) in aqueous solutions with varying NaCl concentrations.

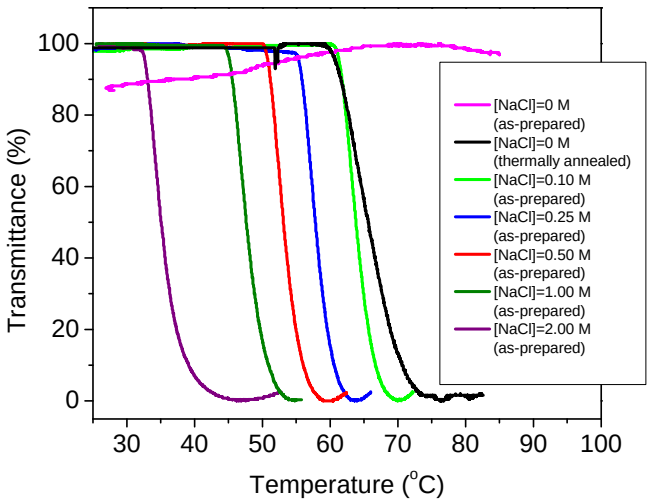

Figure S15. Transmittance versus temperature plots of the polypeptoid bottlebrush [$PNor_{25}$-*g*-P(NEG_{36}-*r*-NBG_{12})] (Entry 3, Table 1) in aqueous solutions with varying NaCl concentrations. The solutions are either subjected to the turbidity measurement directly (as-prepared) or thermally annealed at 75 °C for 10 min followed by cooling at 4 °C overnight prior to the turbidity measurement.

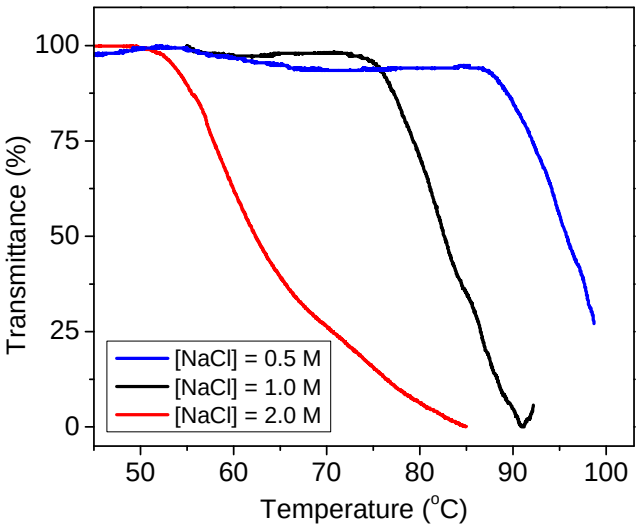

Figure S16. Transmittance versus temperature plots of the polypeptoid macromonomer (Nor-P(NEG_{40}-*r*-NBG_9) (Entry 4, Table S1) in aqueous solutions with varying NaCl concentrations.

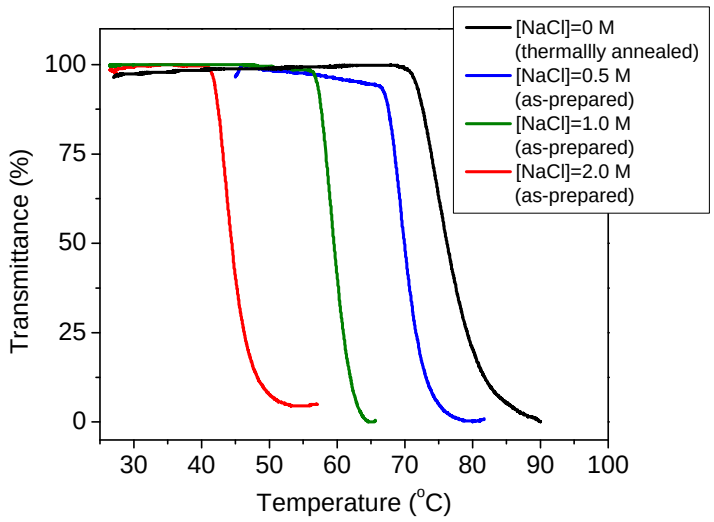

Figure S17. Transmittance versus temperature plots of the polypeptoid bottlebrush [$PNor_{25}$-*g*-$P(NEG_{40}$-*r*-$NBG_9)$] (Entry 5, Table 1) in aqueous solutions with varying NaCl concentrations. The solutions are either subjected to the turbidity measurement directly (as-prepared) or thermally annealed at 75 °C for 10 min followed by cooling at 4 °C overnight prior to the turbidity measurement.

Table S2. T_{cp} and the T_{cp} transition window (TW) of polypeptoid macromonomers [Nor-$P(NEG_m$-*r*-NBG_n)] in aqueous solutions with varying NaCl concentrations.

Entry	Macromonomer composition	[NaCl]	T_{cp} (°C) [a]	TW (°C) [b]
1	Nor-$P(NEG_{27}$-*r*-$NBG_{21})$	0.5	34.2	13.6
		0.25	37.5	12.9
		0.1	39.1	15.3
		0.01	40.4	18.3
		0.0	40.1	14.7
2	Nor-$P(NEG_{37}$-*r*-$NBG_{16})$	0.50	47.7	16.6
		0.25	54.6	21.8
		0.0	62.1	11.5
3	Nor-$P(NEG_{36}$-*r*-$NBG_{12})$	2.0	44.2	16.9
		1.0	59.9	12.3
		0.5	69.4	16.3
4	Nor-$P(NEG_{40}$-*r*-$NBG_9)$	2.0	62.4	22.7
		1.0	75.5	12.0
		0.5	95.8	- [c]

[a.] Determined by turbidity measurements using an optical microscope. T_{cp}s were considered to be the temperature at 50% transmittance; [b.] T_{cp} transition window (TW) is the temperature at 10% transmittance minus the temperature at 90% transmittance; [c.] TW could not be accurately obtained.

Table S3. T_{cp} and the T_{cp} transition window (TW) of polypeptoid bottlebrushes [$PNor_x$-*g*-P(NEG_m-*r*-NBG_n)] (Entry 1-3 and 5, Table 1) in aqueous solutions with varying NaCl concentrations.

Entry	Bottlebrush composition	[NaCl]	T_{cp} (^oC) [a]	TW (^oC) [b]
1	$PNor_{25}$-*g*-P(NEG_{27}-*r*-NBG_{21})	0.25	32.4	4.8
		0.1	34.1	4
		0.01	37	16.3
		0.0	37.3	24.6
2	$PNor_{25}$-*g*-P(NEG_{37}-*r*-NBG_{16})	1	35.3	4.3
		0.5	41.5	4.6
		0.25	43.2	5.1
		0.0	47.2	9.2
3	$PNor_{25}$-*g*-P(NEG_{36}-*r*-NBG_{12})	2	35.1	6
		1	47.6	8.4
		0.5	53.1	4.8
		0.25	57.8	4.8
		0.1	63.8	5
		0.0	65.6	13
4	$PNor_{25}$-*g*-P(NEG_{40}-*r*-NBG_9)	1	59.5	4.7
		0.5	69.9	6.3
		2	44.4	6.7
		0.0	78.8	18.8

[a.] Determined by turbidity measurements using an optical microscope. T_{cp}s were considered to be the temperature at 50% transmittance; [b.] T_{cp} transition window (TW) is the temperature at 10% transmittance minus the temperature at 90% transmittance.

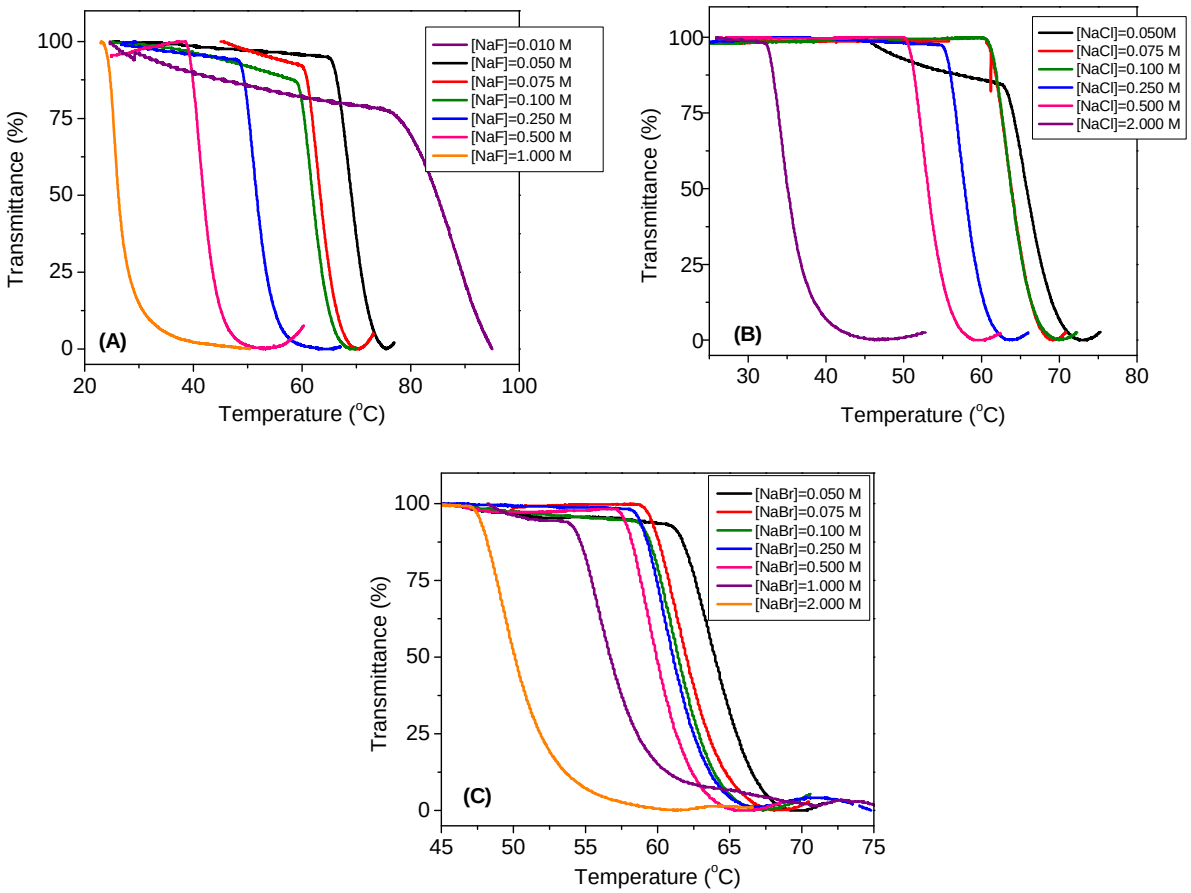

Figure S18. (A) Transmittance versus temperature plots of the polypeptoid bottlebrush [$PNor_{25}$-*g*-$P(NEG_{36}$-*r*-$NBG_{12})$] (Entry 3, Table 1) in aqueous solutions with varying NaF, (B) NaCl and (C) NaBr concentrations.

Table S4. T_{cp} of the polypeptoid bottlebrush $PNor_{25}$-*g*-$P(NEG_{36}$-*r*-$NBG_{12})$ (Entry 3, Table 1) in aqueous solutions with various inorganic salt concentrations

[Salt] (M)	T_{cp}^{NaCl} (°C) [a]	T_{cp}^{NaF} (°C) [a]	T_{cp}^{NaBr} (°C) [a]
0.05	-- [c]	-- [c]	64
0.075	-- [c]	63.4	-- [c]
0.1	63.8	61.9	-- [c]
0.25	57.8	51.6	61.1
0.5	53.1	41.9	59.9
1.0	47.6	26.2	56.7
2.0	35.1	-- [b]	50.1

[a.] Determined by turbidity measurements using an optical microscope. T_{cp}s were considered to be the temperature at 50% transmittance; [b.] samples were not soluble in the corresponding NaCl/H_2O solution at room temperature; [c.] samples were not analyzed by turbidity measurements at the given salt concentration.

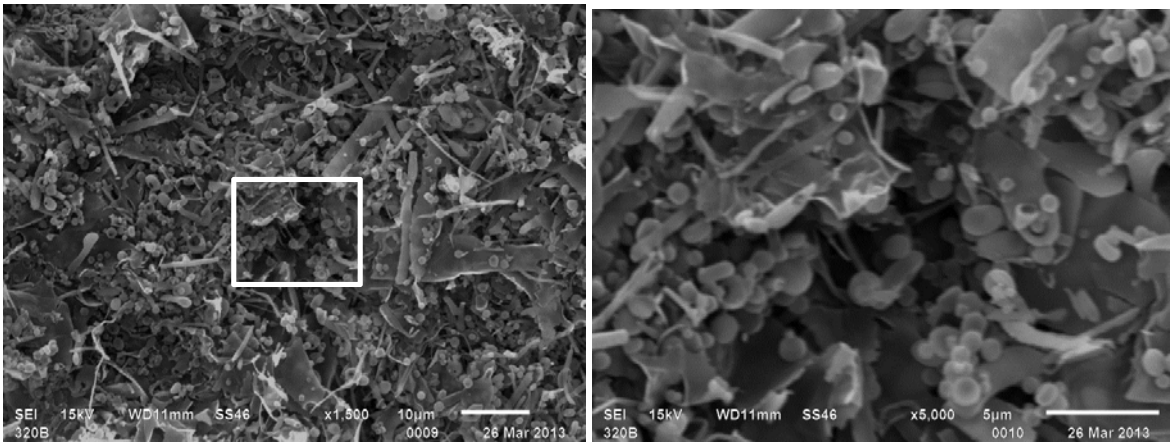

Figure S19. (A) Full and (B) expanded SEM images of the bottlebrush copolymers [$PNor_{25}$-*g*-$P(NEG_{40}$-*r*-$NBG_9)$] that precipitated from the aqueous solution after being held at 80 °C overnight. The sample used in SEM analysis was obtained by lyophilizing a 2.0 mg·mL^{-1} polymer suspension.

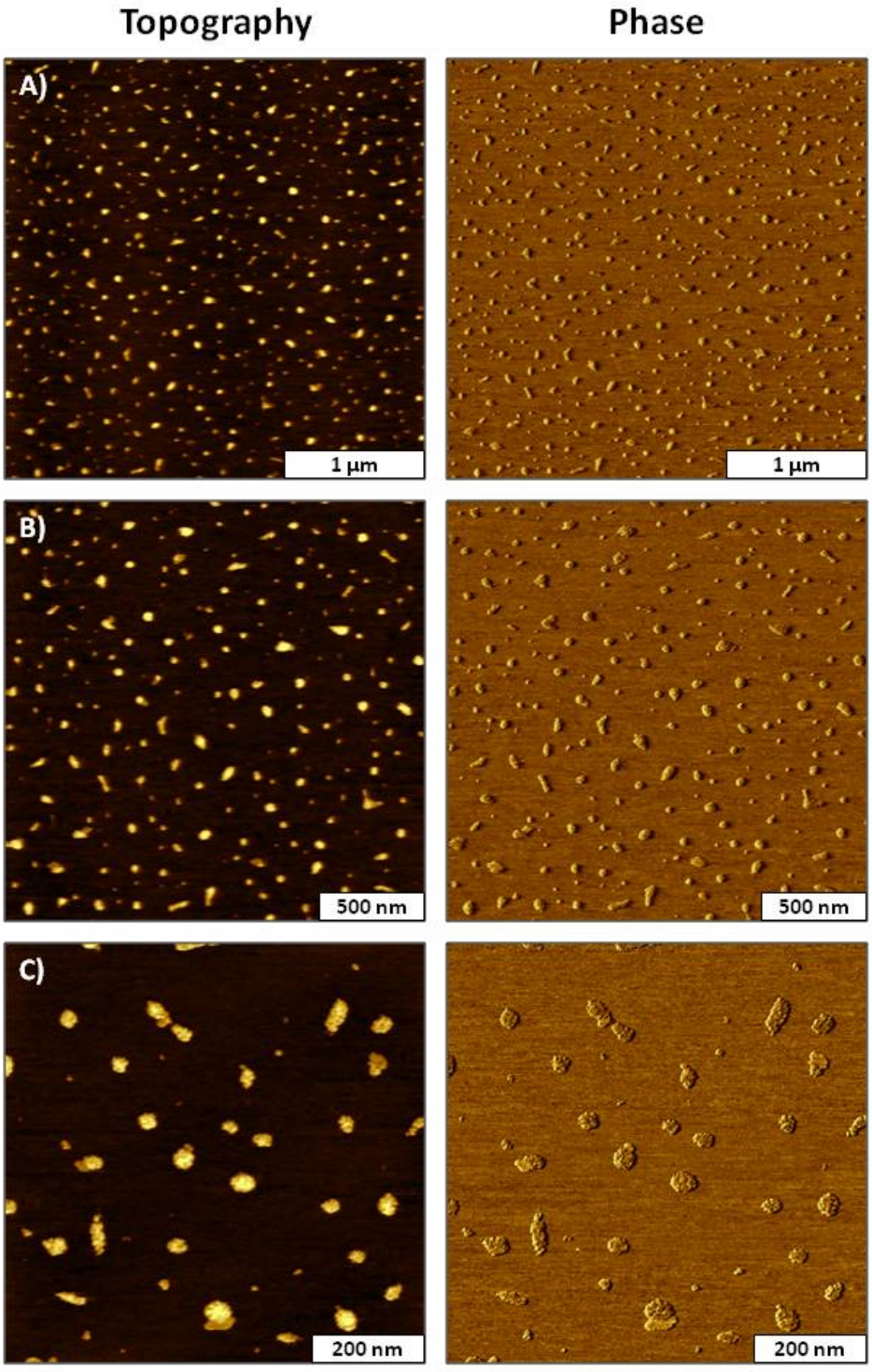

Figure S20. The shapes and distributions of bottlebrush polypeptoids sample $PNor_{150}$-*g*-P(NEG_{36}-*r*-NBG_{12}) (Entry 4, Table 1) viewed with AFM. Topographs and corresponding phase images of (A) 6 × 6 um^2; (B) 4 × 4 um^2; (C) 1.5 × 1.5 um^2 areas.